

1     **A hierarchically acidity-unlocking nanoSTING stimulant**  
2     **enables cascaded STING activation for potent innate and**  
3             **adaptive antitumor immunity**

4     Shunyao Zhu<sup>1,+</sup>, Tao He<sup>1,+</sup>, Yan Wang<sup>1</sup>, Yushan Ma<sup>2,3</sup>, Wenmei Li<sup>4</sup>, Songlin Gong<sup>1</sup>,  
5     Yanghui Zhu<sup>1</sup>, Xiangwei Wang<sup>1</sup>, Xu Xu<sup>5</sup>, Qinjie Wu<sup>1</sup>, Changyang Gong<sup>1,\*</sup>, Yanjie  
6     You<sup>2,3,\*</sup>

7     <sup>1</sup> Department of Biotherapy, Cancer Center and State Key Laboratory of Biotherapy,  
8     West China Hospital, Sichuan University, Chengdu, 610041, China

9     <sup>2</sup> Department of Gastroenterology, the Third Clinical Medical College of Ningxia  
10    Medical University, Yinchuan, 750002, China

11    <sup>3</sup> Department of Gastroenterology, People's Hospital of Ningxia Hui Autonomous  
12    Region, Yinchuan, 750002, China

13    <sup>4</sup> Department of Clinical Laboratory Medicine, People's Hospital of Ningxia Hui  
14    Autonomous Region, Ningxia Medical University, Ningxia Hui Autonomous Region,  
15    Yinchuan, 750002, China

16    <sup>5</sup> School of Pharmacy, Henan University, Kaifeng, 475004, China

17    \* To whom correspondence should be addressed (C Gong and Y You), E-mail:  
18    chyong14@163.com and youyanjie@163.com.

19    <sup>+</sup> These authors contributed equally to this work.

20 Table S1 List of antibodies applied to flow cytometric analysis.

Antibody	Clone	Fluorophore	Source	
CD3	17A2	PE-cy7	Biolegend	
CD3	17A2	APC/Cyanine5	Biolegend	
CD4	GK1.5	PE	Biolegend	
CD45	QA17A26	APC	Biolegend	
CD8a	53-6.7	FITC	Biolegend	
CD8a	53-6.7	PE/Cyanine5	Biolegend	
CD80	16-10A1	APC	Biolegend	
CD86	GL-1	PE-cy7	Biolegend	
CD69	H1.2F3	PE	Biolegend	
CD25	3C7	FITC	Biolegend	
CD11b	M1/70	FITC	Biolegend	
NK1.1	S17016D	PE	Biolegend	
CD44	IM7	FITC	Biolegend	
CD62L	MEL-14	APC	Biolegend	
Foxp3	FJK-16s	APC	eBioscience	
CD16/32 (Fc Block)	93	--	eBioscience	
$\gamma$ H2AX	S139	--	Abcam	
dsDNA	J2	--	Cell Technology	Signaling
STING	Ser365	--	Cell Technology	Signaling
p-STING	Ser366	--	Cell Technology	Signaling
IRF3	D83B9	--	Cell Technology	Signaling
p-IRF3	SER396	--	Cell	Signaling

---

			Technology	
TBK1	D1B4	--	Cell Technology	Signaling
p-TBK1	Ser172	--	Cell Technology	Signaling
GAPDH	D4C6R	--	Cell Technology	Signaling

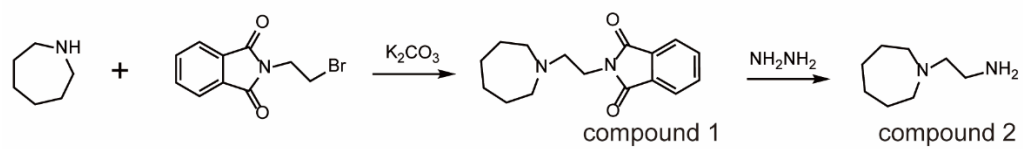
---

21

22 Table S2 The long-term stability of AUG at 4 °C (n = 3).

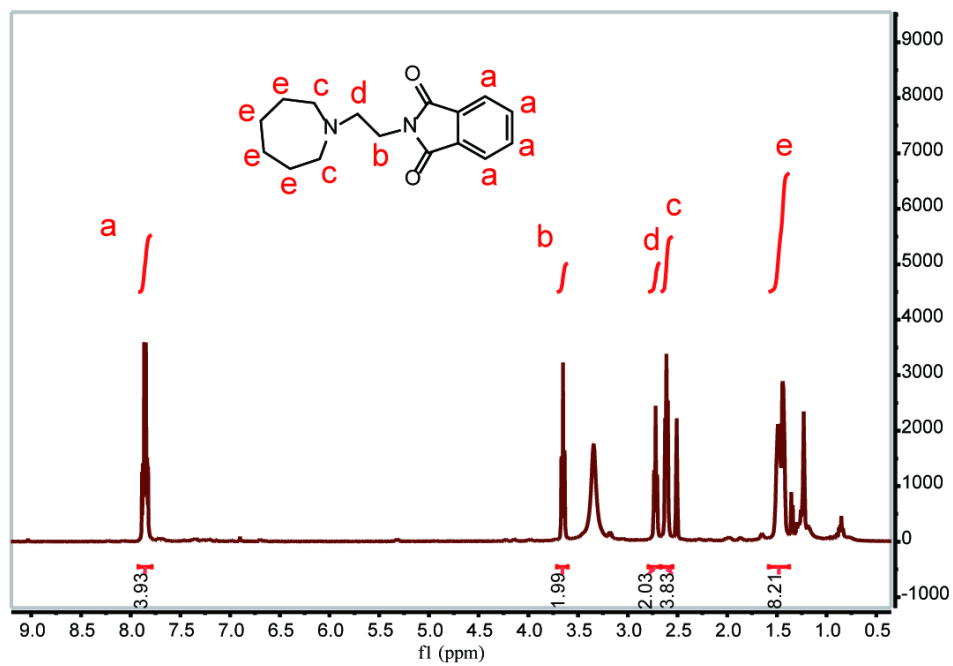
	Size (nm)	Polymer dispersity index (PDI)	Zeta potential (mV)	Doxorubicin (%)
0 Day	152.4 ± 1.6	0.218 ± 0.023	-10.42 ± 1.07	100.0 ± 0.3
7 Day	154.7 ± 2.9	0.168 ± 0.019	-4.51 ± 0.16	99.7 ± 0.9
14 Day	154.1 ± 3.0	0.144 ± 0.018	-6.49 ± 0.43	98.6 ± 1.3
21 Day	154.7 ± 0.4	0.167 ± 0.009	-5.17 ± 1.24	99.2 ± 0.8
28 Day	155.3 ± 1.0	0.161 ± 0.008	-4.16 ± 0.76	99.4 ± 1.0

23



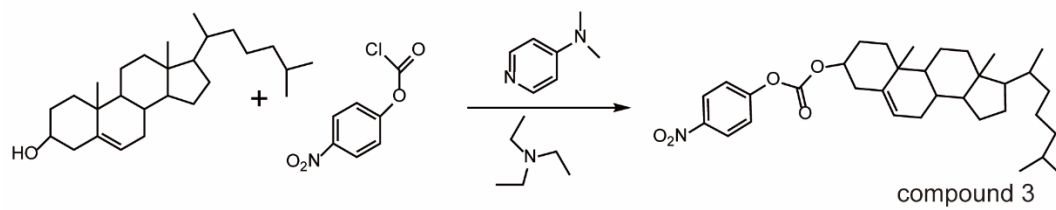
24

25 Figure S1. The synthesis routes of C7A-NH<sub>2</sub> (compound 2).



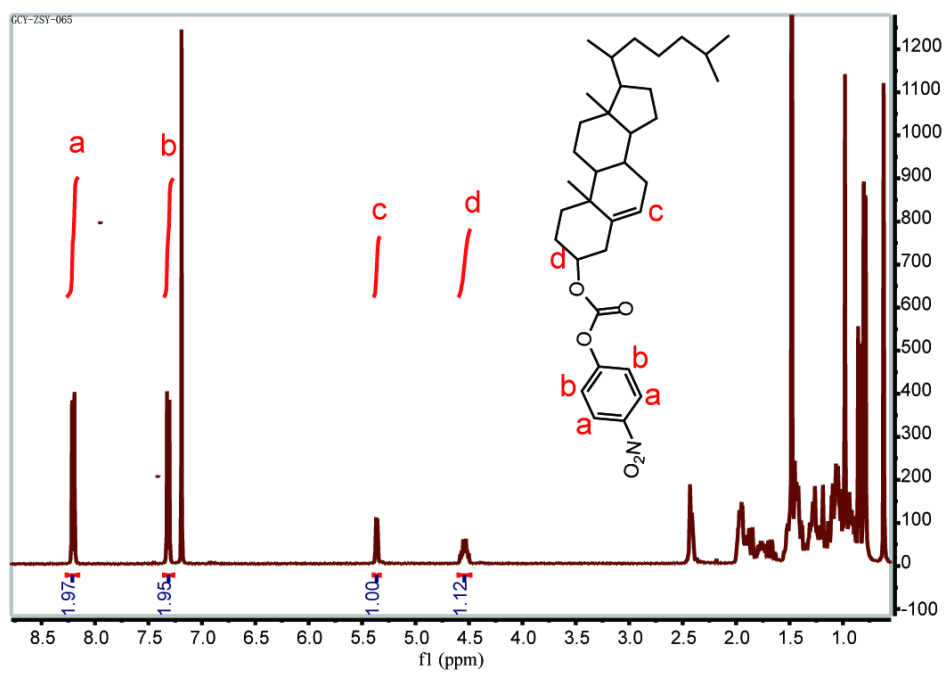
26

27 Figure S2. <sup>1</sup>H NMR spectrums of compound 1.



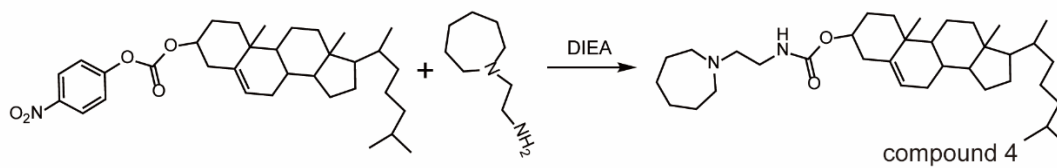
28

29 Figure S3. The synthesis routes of CHOL-COOR.



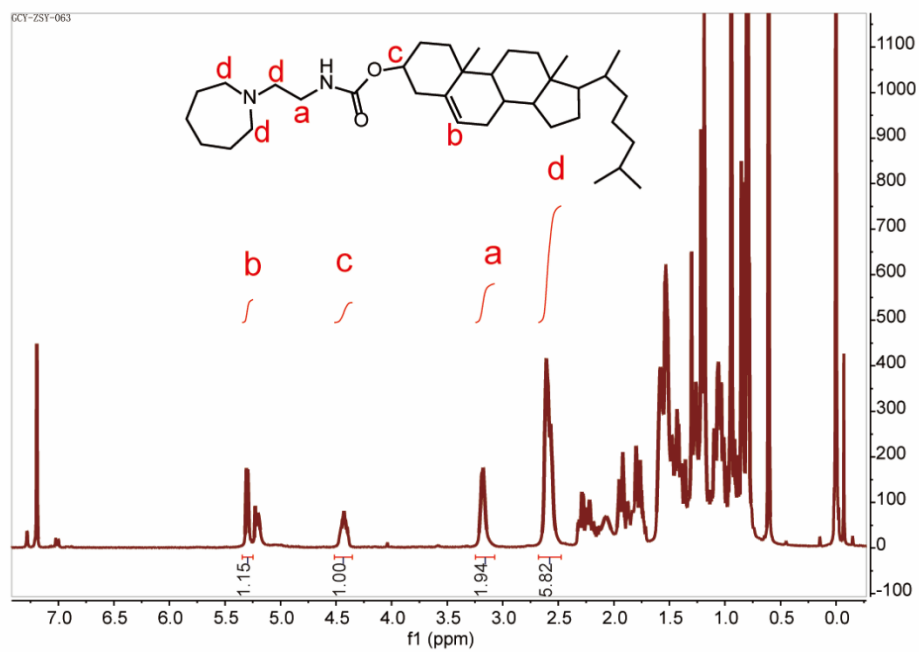
30

31 Figure S4. <sup>1</sup>H NMR spectrums of CHOL-COOR



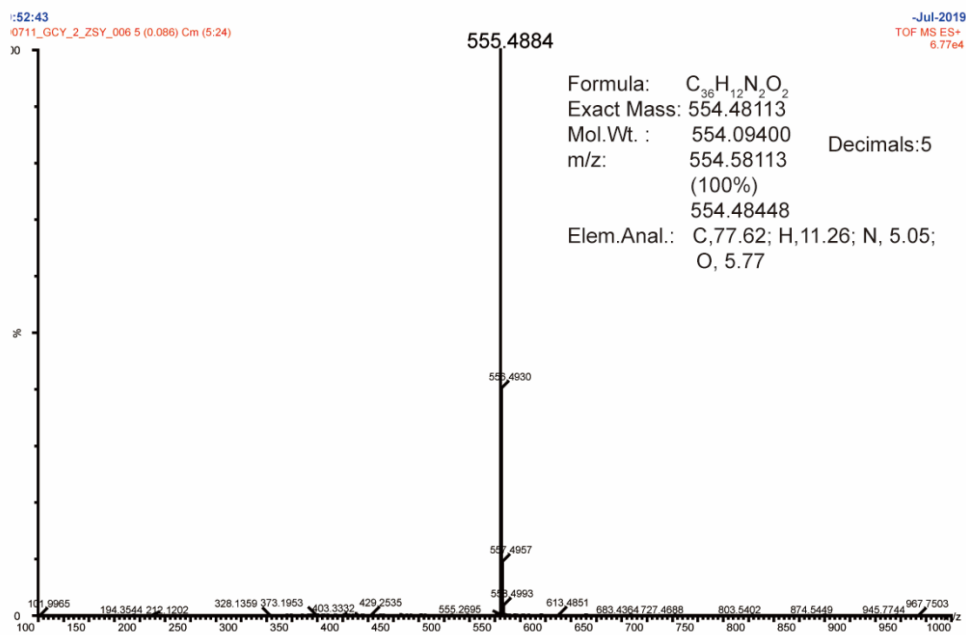
32

33 Figure S5. The synthesis routes of CHOL-C7A.



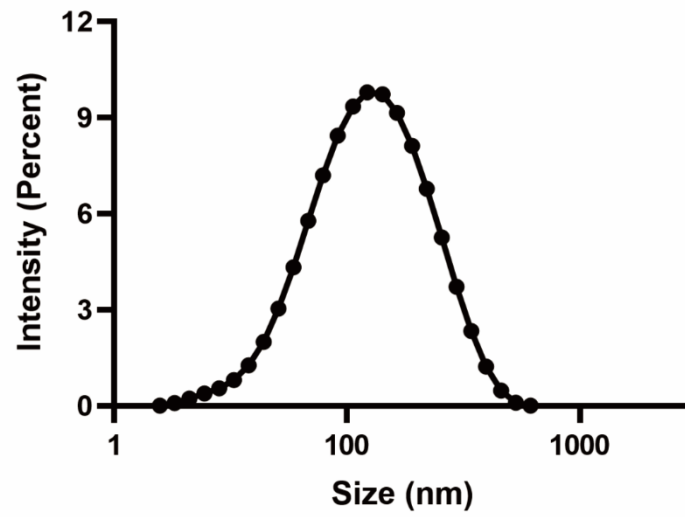
34

35 Figure S6. <sup>1</sup>H NMR spectrums of compound CHOL-C7A.



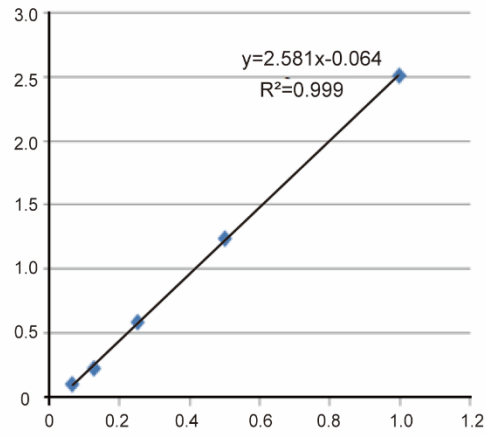
36

37 Figure S7. MS spectra of CHOL-C7A.



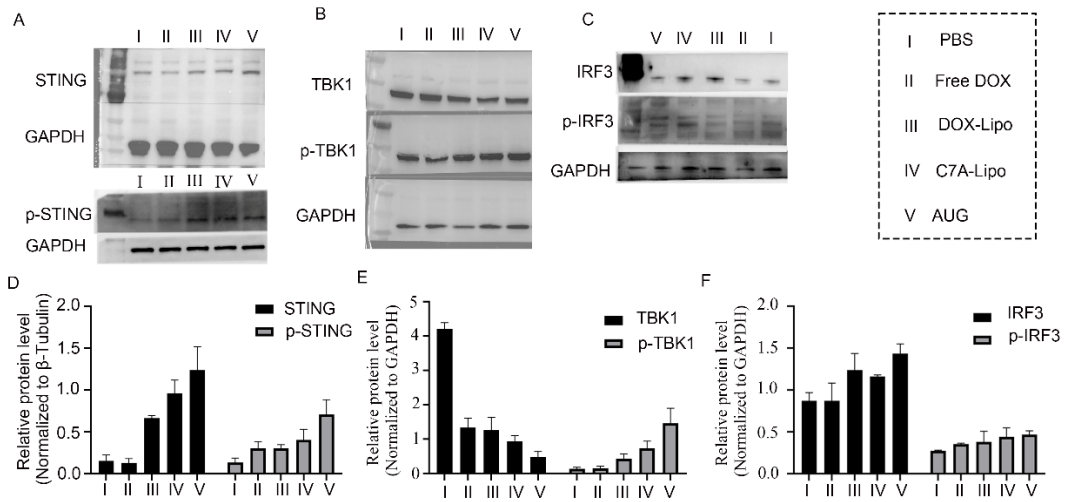
38

39 Figure S8. Size distribution of C7A-Lipo at pH 7.4.



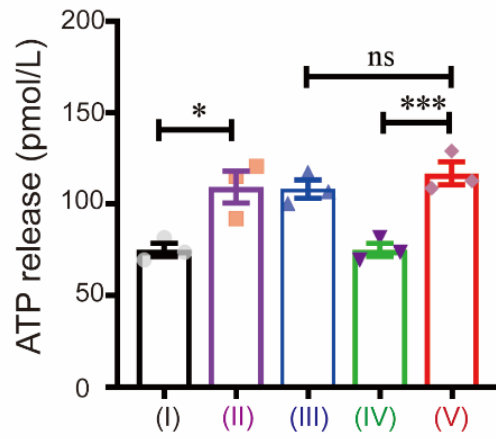
40

41 Figure S9. The standard curve was prepared by CHOL-C7A.



42

43 Figure S10. Representative gel image and quantitative statistics of (A) STING and p-  
 44 STING; (B) TBK1 and p-TBK1. (C) IRF3 and p-IRF3 proteins expression in B16-F10  
 45 cells within different treatments.

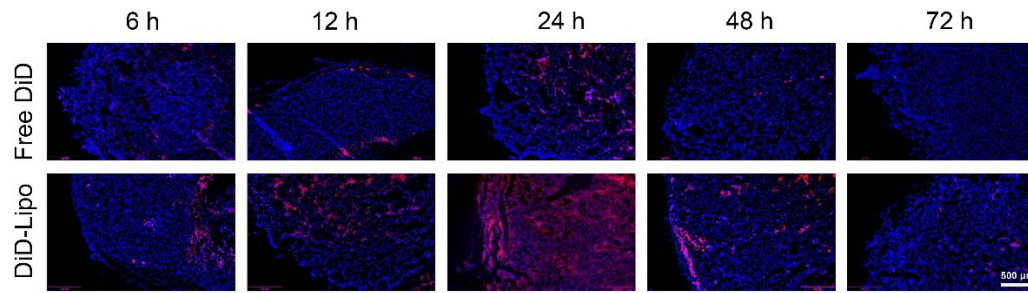


46

47 Figure S11. Quantification of ATP released from B16-F10 cell induced by DOX (n =

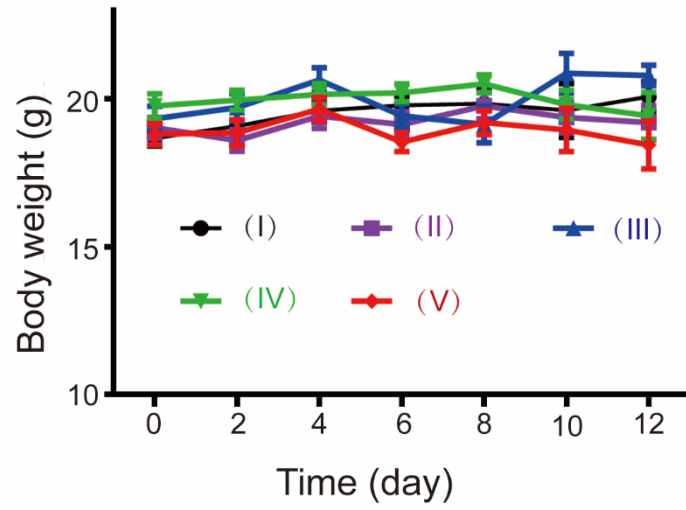
48 3). (I) PBS; (II) Free DOX; (III) DOX-Lipo; (IV) C7A-Lipo and (V) AUG. Data are

49 means  $\pm$  SD. \* $P < 0.05$ , \*\* $P < 0.01$ , \*\*\* $P < 0.001$  determined by Student's t-test.



50

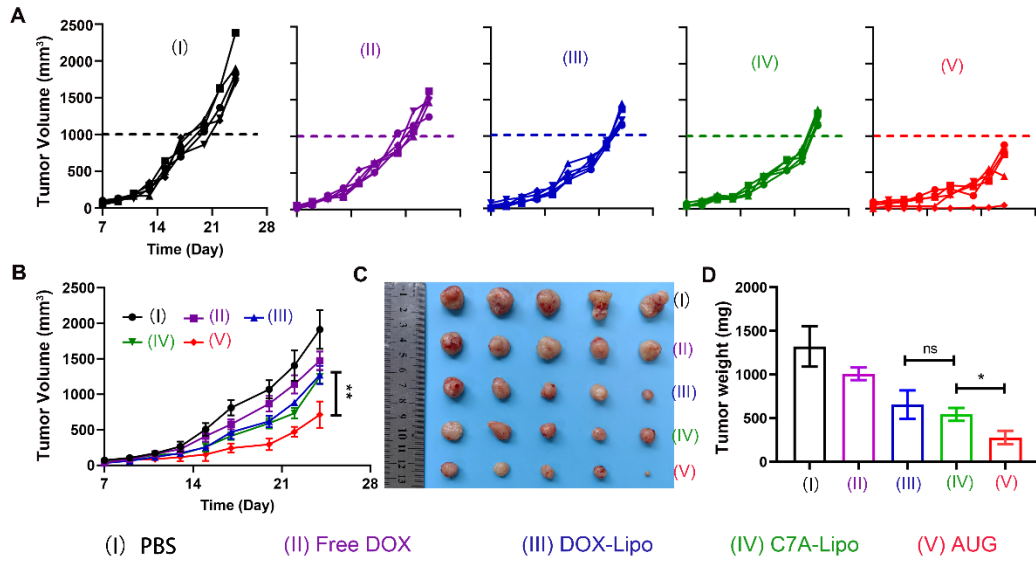
51 Figure S12. Representative fluorescence images depicting the infiltration and  
52 subsequent elimination of the therapeutic agent AUG within tumor tissues, with AUG  
53 being fluorescently labeled with DiD for enhanced visualization. Scale bar: 500  $\mu\text{m}$ .



54

55 Figure S13. Changes of body weight during the treatment (n = 3). (I) PBS; (II) Free

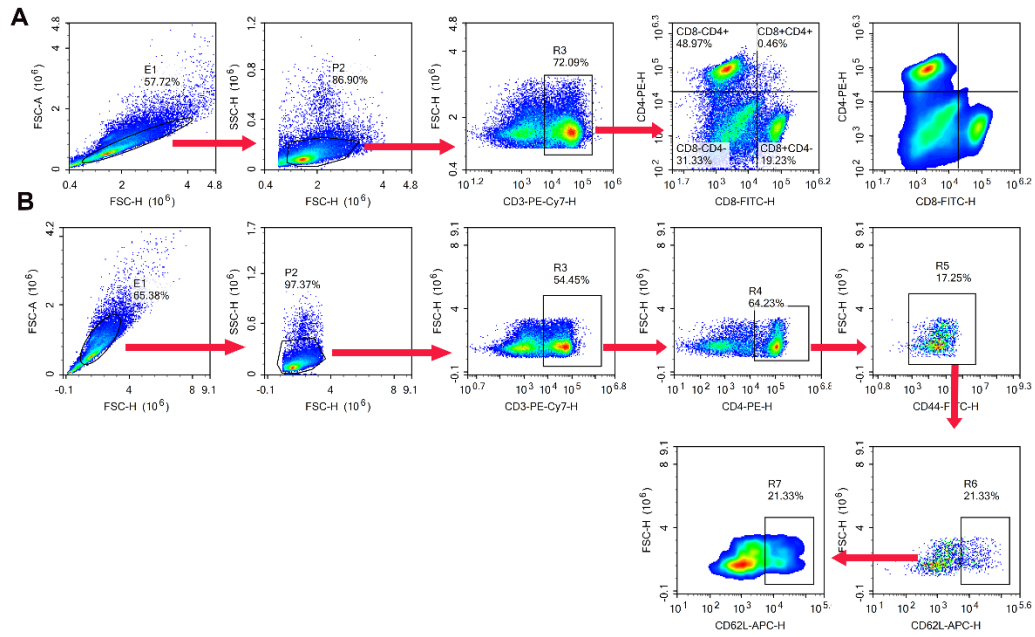
56 DOX; (III) DOX-Lipo; (IV) C7A-Lipo and (V) AUG.



57

58 Figure S14: The antitumor effect of AUG in MC38 tumor. (A) Tumor growth curves  
 59 for each mouse. (B) Total tumor growth curves of mice in different groups post-  
 60 treatment. (C and D) Photographs of dissected tumors (C) and average tumor weights  
 61 (D) at the end of the treatment. Ns = non-significant, \* $P < 0.05$ , \*\* $P < 0.01$ , \*\*\* $P <$   
 62 0.001.



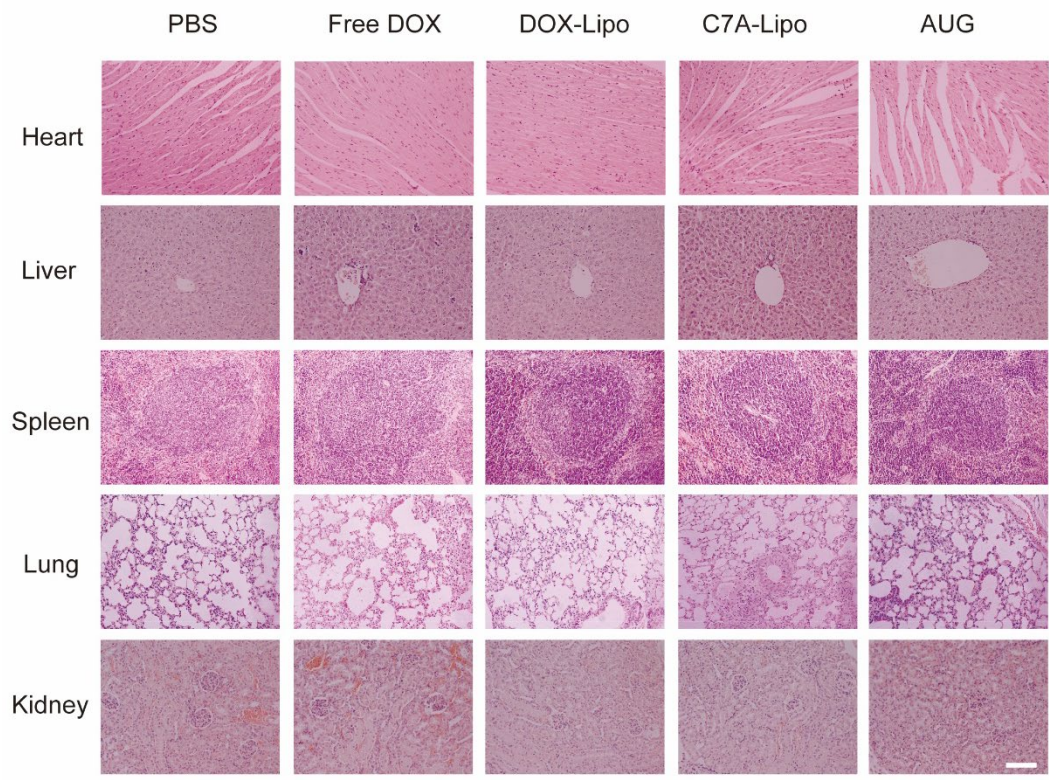


70

71 Figure S16. The gating strategy for manual analysis to sequentially identify the

72 proportion of CD4<sup>+</sup>/CD8<sup>+</sup> (A) and CD62L<sup>+</sup> (B) expressed in the spleen. Note: the

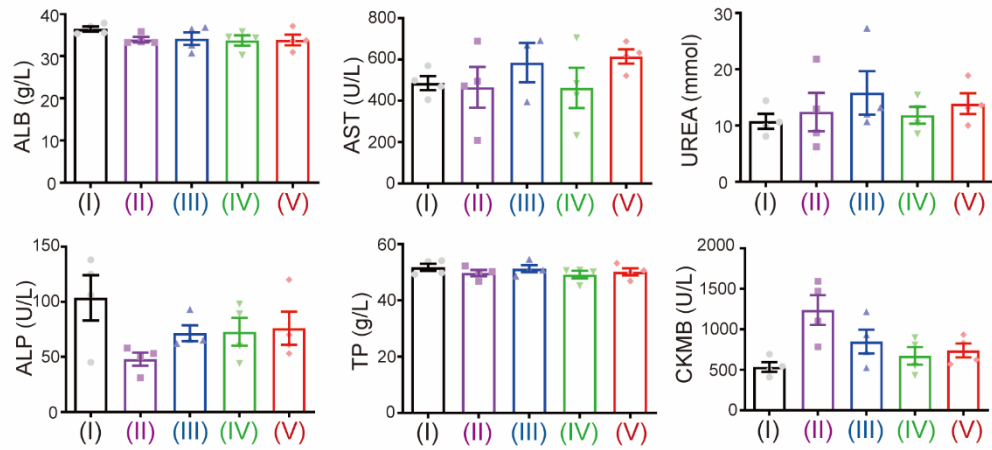
73 percentages shown represent the frequency of cells relative to the parent gate.



74

75 Figure S17. H&E staining of tissues including heart, liver, spleen, lung and kidney from

76 C57BL/6 mice after various formulation treatment. The scale bar is 100  $\mu$ m.



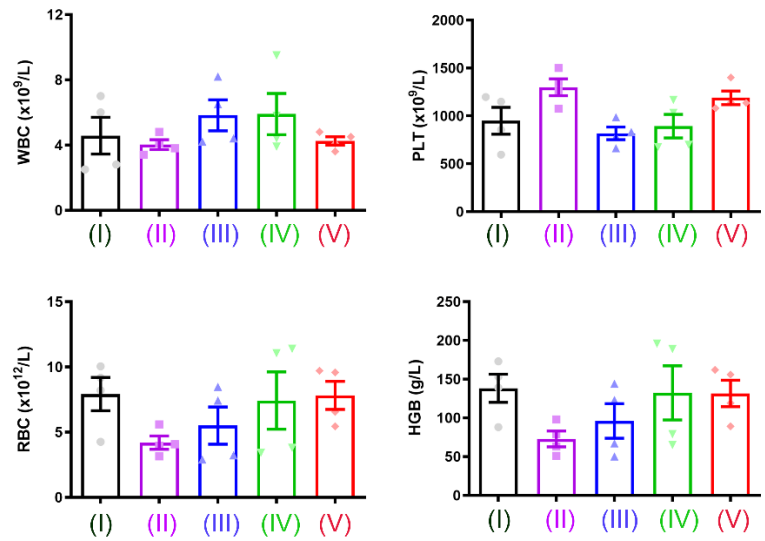
77

78 Figure S18. Serum chemistry levels in mice, including ALB, AST, UREA, ALP, TP and

79 CKMB. (I) PBS; (II) Free DOX; (III) DOX-Lipo; (IV) C7A-Lipo and (V) AUG (n = 4).

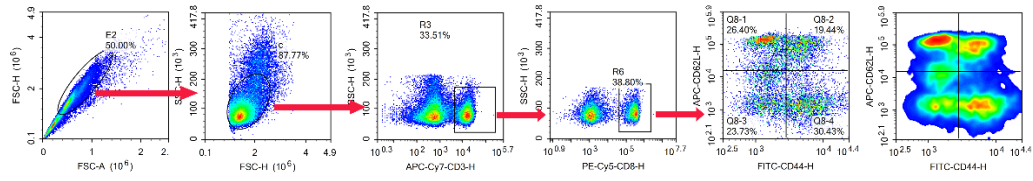
80 Data are means  $\pm$  SD. \* $P < 0.05$ , \*\* $P < 0.01$ , \*\*\* $P < 0.001$  determined by Student's t-

81 test.



82

83 Figure S19. Blood routine levels in mice after treatment, including WBC, RBC, HGB  
 84 and PLT. (I) PBS; (II) Free DOX; (III) DOX-Lipo; (IV) C7A-Lipo and (V) AUG (n =  
 85 4). Data are means  $\pm$  SD. \* $P < 0.05$ , \*\* $P < 0.01$ , \*\*\* $P < 0.001$  determined by Student's  
 86 t-test.



87

88 Figure S20. The gating strategy for manual analysis to sequentially identify the  
 89 proportion of  $T_{CM}$  and  $T_{EM}$  cells in the spleen. Note: the percentages shown represent  
 90 the frequency of cells relative to the parent gate.